

# Quantifying the effects of TTI in multiphysics analysis of electromagnetic data offshore Malaysia

Randall Mackie\* (Viridien), Lucy MacGregor, Ahmad Shahir Saleh, and Joanna Kho (Petronas)

## Summary

Marine sediments are often electrically anisotropic at a scale that affects controlled source electromagnetic (CSEM) data. When the sedimentary sequence is steeply dipping, it is important to model the data using resistivity fields that follow the sedimentary bedding, which is called tilted transverse isotropy (TTI). In this paper, we introduce our approach to the inversion of CSEM data in TTI media, which builds on our previous work using seismic-guided inversion. We illustrate this with synthetic examples representative of the geological settings encountered in Sabah and show how results impact data analysis in the area.

## Introduction

Multiphysics approaches combining seismic with non-seismic information from electromagnetic surveys have been shown to improve the robustness of subsurface characterization and can be applied to both exploration and appraisal challenges. There is a large database of controlled source electromagnetic (CSEM) and magnetotelluric (MT) data from offshore Sabah and Sarawak in Malaysia. This data has been used for both regional understanding (Meju et al., 2024; Kho et al., 2024) and prospect-level characterization (Karpiah et al., 2022; Saleh et al., 2023). CSEM and MT methods are sensitive to the electrical resistivity of the subsurface. Electrical anisotropy is a first-order effect, and while vertical to horizontal anisotropy ratios of two are typically observed, ratios of ten or more can be found in certain sediments (such as those that have been compacted at depth and uplifted, e.g., Alvarez et al., 2017).

Most of the data analysis conducted so far in Malaysia has assumed vertical transverse isotropy (VTI), in which two resistivity values are defined: the horizontal resistivity, which does not vary with azimuth, and the vertical resistivity, which is usually higher. This approximation works well in relatively flat lying sediments; however, in dipping sediments, more accurate results are obtained if we assume tilted transverse isotropy (TTI) (e.g., Hansen et al., 2016; BJORKE et al., 2020). Here, the resistivity is again defined by two values; however, these are now bed-parallel (transverse resistivity) and bed-perpendicular (normal resistivity), allowing the anisotropy to follow stratigraphy. Interpretations that assume a VTI medium when the underlying medium is TTI can lead to artifacts in the results, which in turn lead to greater uncertainty in interpretation of subsurface features (Hansen et al., 2018).

In Malaysia, there are several geological settings where TTI may have a significant impact on the interpretation. Here, we concentrate on one of these: the thrust belts encountered offshore Sabah, where steeply dipping sediments are encountered (Saleh et al., 2023). We first introduce our approach to the inversion of CSEM and/or MT data in TTI media, which builds on the seismic-guided inversion approach of Mackie et al. (2020). We illustrate this firstly with synthetic examples representative of the geological settings encountered in Sabah, and then we discuss the impact that TTI has on the interpretation of multiphysics data in the region.

## Theory and Method

The multiphysics software suite used in this study (e.g., Mackie et al., 2020; Soyer et al., 2020; Hoversten et al., 2021) includes capabilities to model and invert a range of geophysical data including frequency-domain electromagnetic data such as CSEM and MT, gravity, gravity gradiometry, magnetics, and seismic travel times. The anisotropic inversions of CSEM and/or MT were previously based on the VTI assumption implemented using a staggered-grid Finite Integration Technique (Weiland, 1977). Recently, we extended the capability to handle TTI models, implemented following the approach of Weiss and Newman (2002), which interpolates edge-based electric field values to required positions using volume-averaging for needed conductivity values, thereby maintaining the current grids used for VTI modeling.

Modeling a TTI geometry requires four parameters in each model cell: transverse and normal resistivities, and anisotropy strike and dip angles. In this work, we take the anisotropy strike and dip angles to be fixed, computed from 3D seismic; in this way, the anisotropy strike and dip angles are consistent with the seismic structure.

## Synthetic examples

We first consider a simple 2D model of an anticline (Figure 1, top row) in which the TTI dip is 30 degrees to the horizontal on the flanks and zero at the axis of the structure (see top left panel of Figure 4). An anisotropy ratio of 3 is assumed within the anticline, and for simplicity, the background resistivity is taken to be isotropic. Synthetic CSEM data from across strike tow lines was generated at 0.2, 0.6, and 1.2 Hz, assuming a 1 km grid of receivers at the seafloor, and contaminated with representative Gaussian noise. Figure 1 (middle and bottom rows) compares results

## TTI CSEM inversion

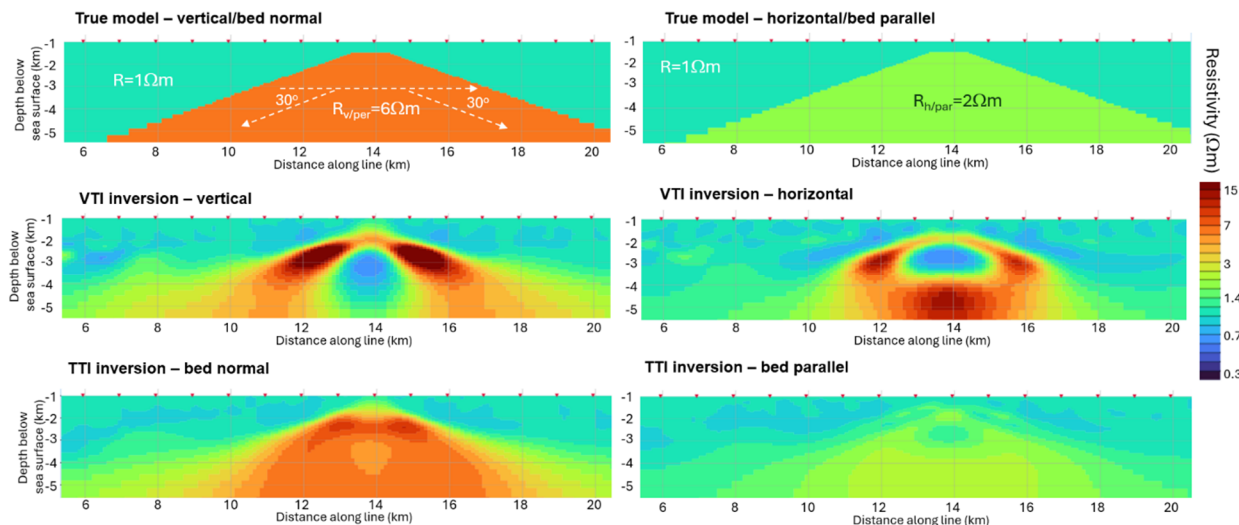


Figure 1: Top row: simple resistivity model representing an anticline with flanks dipping at 30 degrees to the horizontal. Middle row: inversion of TTI synthetic data using a VTI assumption leads to clear artifacts in the result. Bottom row: TTI inversion with the correct dip and strike leads to a good image of the input model.

inverted using both an incorrect VTI assumption and with the correct TTI dip and strike angles. As observed in previous studies (e.g., Hansen et al., 2018), significant artifacts are observed when an incorrect VTI assumption is made. These are minimal/absent in the TTI inversion.

The TTI dip and strike are fixed in the inversion. It is therefore important to assess how an error in these parameters affects the measured response. Models with dip angles on the left-hand side of the anticline between 10 and 50 degrees were constructed, and the response of these compared to the response of the model shown in the top row of Figure 1. These results are shown in Figure 2, which plots the percentage change in amplitude and phase difference for each model, compared to the response of the symmetric 30-degree dip model. Even an error of 5 degrees in the dip angle could lead to change of up to 5% in the measured response. For good quality CSEM data, this would be above the noise floor and therefore significant. Results are shown for a 0.2 Hz transmission frequency. Differences increase for higher frequency data. In contrast, an error in strike of up to 20 degrees is required to give a measurable change in the response. This highlights the importance of correctly characterizing the dip angle.

### Field data example

Figure 3 compares VTI and TTI inversion of real data from the offshore area of Sabah, Malaysia where structural dip is estimated to be up to 60 degrees. For the TTI inversion, dip

and strike angles were built from seismic depth horizons as this gave a more stable and less noisy result than when calculated directly from seismic reflectivities. The VTI inversion is very clearly contaminated with artifacts. In contrast, the TTI inversion is much more stable and conforms better to structure. Both inversions fit the data to a root mean square misfit of 1.3; however, the TTI converged to this value in 40 iterations, while the VTI inversion took 50 iterations.

Looking in more detail at the TTI inversion results, there is an area of low resistivity and low anisotropy with poorer structural conformance on the sub-thrust side of the structure (circled in cyan on the anisotropy plot in Figure 3). Given the synthetic inversion results suggest that even a small error in dip angle can lead to significant changes in response, a synthetic model was constructed to further investigate this effect (Figure 4). Dip and strike angles were constructed assuming an anticline-like structure (top left panel of Figure 4) and a thrust structure (top right panel of Figure 4). Synthetic data generated from the thrust model were then inverted for a TTI structure assuming the dip model from the anticline structure. The resulting anisotropy model is shown in the bottom panel of Figure 4. A low-anisotropy zone similar to that observed in the inversion of the real data is observed. This suggests that for this complex geology, it is necessary to have the best quality seismic image in order to use the seismically derived dip angles for more robust inversion result.

## TTI CSEM inversion

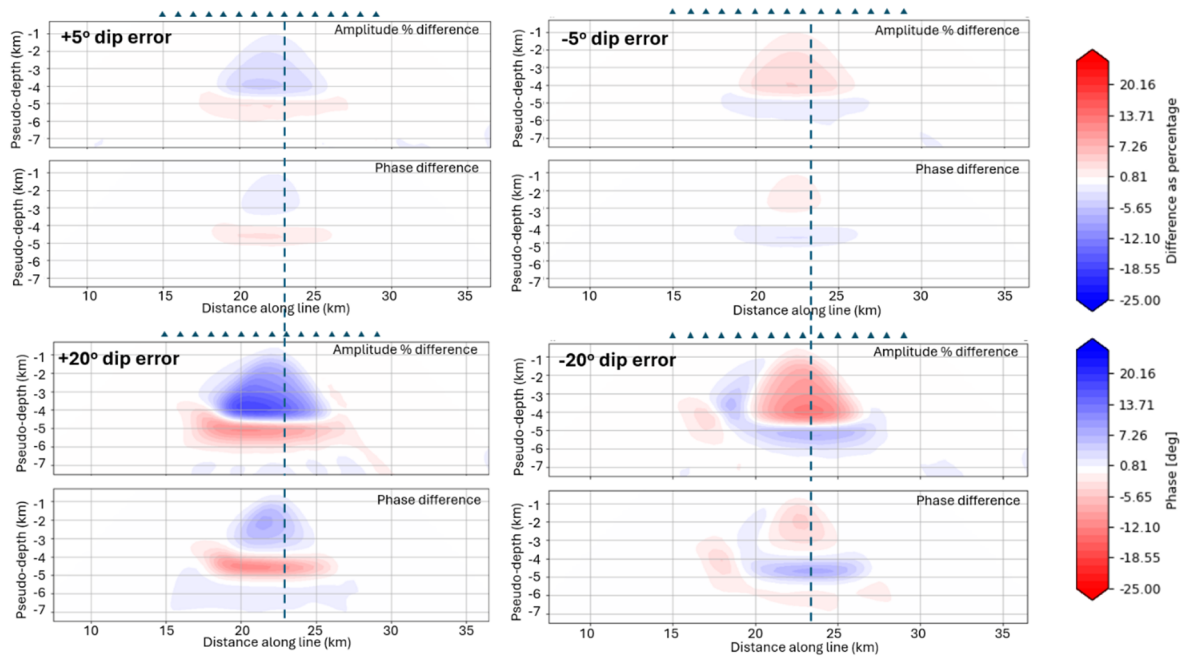


Figure 2: The effect of an incorrect dip angle is illustrated by plotting the % difference in amplitude and absolute phase difference in the inline electric field at 0.2 Hz for a tow line across the anticline structure shown in Figure 1. The dashed line marks the crest of the anticline. The response of a model with dips varying between 10 and 50 degrees on the left-hand flank of the anticline is compared to that of the correct 30-degree dip. Note that the dip on the right-hand flank maintains the correct 30-degree dip in all models. A positive angle error corresponds to a steeper dip than reality.

### Conclusions

Assuming VTI anisotropy in a TTI (dipping) medium has the potential to make interpretation of subsurface features uncertain, or in the worst case, misleading. The results presented here highlight the importance of correctly accounting for TTI electrical anisotropy when using electromagnetic data in multiphysics workflows. Results also show the necessity to have good constraint on seismic structure. In this example, where seismic imaging is poor in the core of the thrust, the TTI result is sub-optimal. Allowing the dip angle to vary in the inversion (as in previously presented TTI inversion such as that of Hansen et al., 2018) may be a solution, and this will be presented in future work. Ongoing development includes application to both land and marine MT data, and other EM methods.

### Acknowledgments

The authors thank PETRONAS and Viridien for permission to present this work.

### TTI CSEM inversion

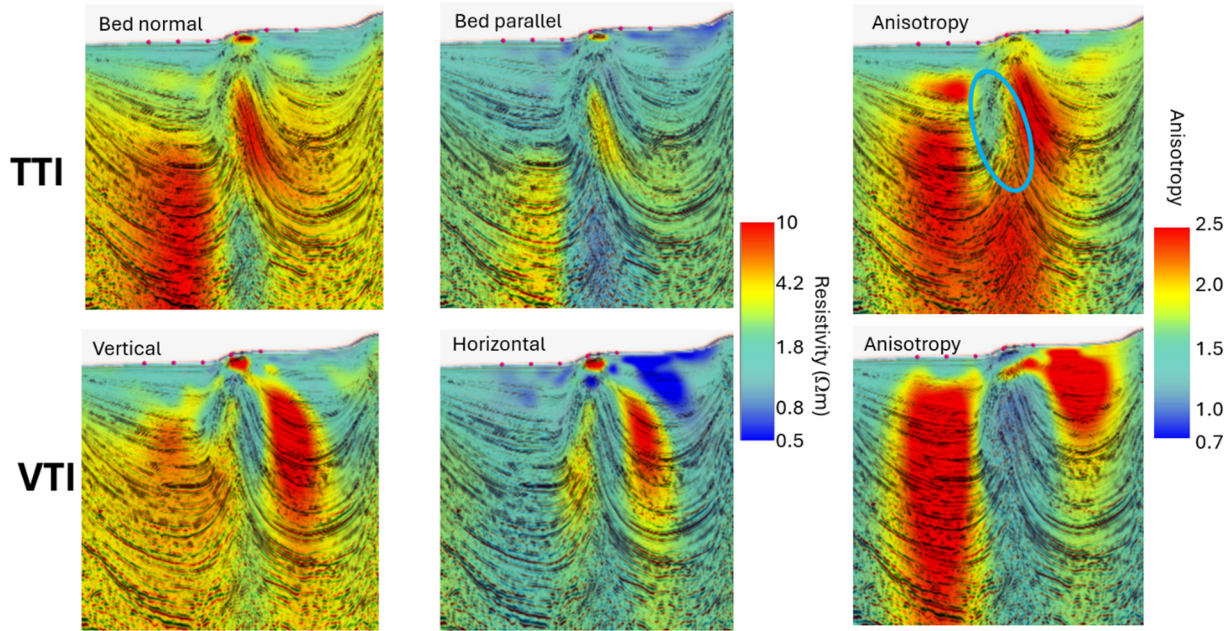


Figure 3: Upper panels: TTI inversion of CSEM data from a thrust structure in Sabah. Overall good structural conformance is observed, although there remains an area of anomalously low resistivity/anisotropy in the sub-thrust area (cyan ellipse). Lower panels: VTI inversion of the same data is clearly contaminated with artifacts.

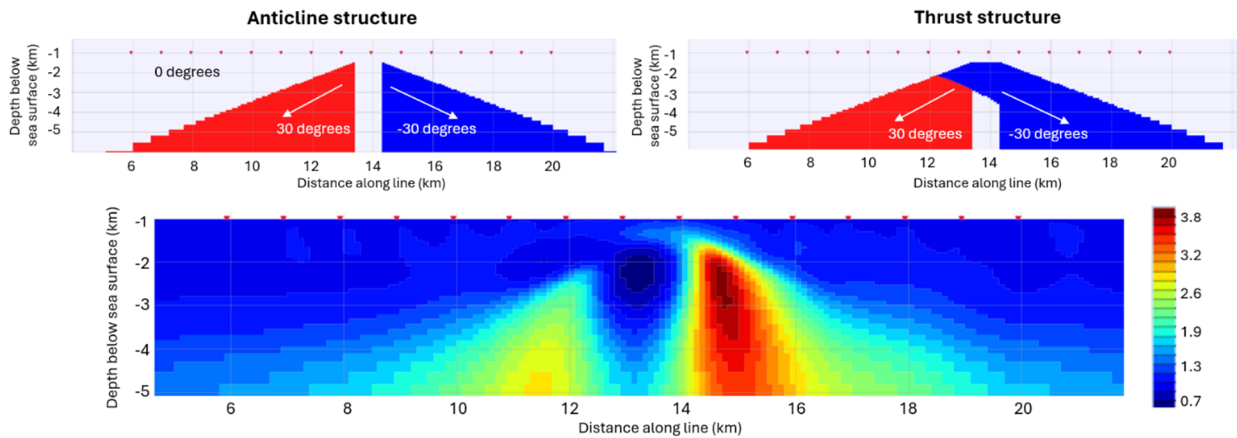


Figure 4: Upper left panel: Dip model for an anticline structure. Dip is symmetric about the crest of the anticline. Upper right panel: Dip model for a thrust structure. The structure is asymmetric about the crest. Seismic data are sufficiently clear in the core of the structure to discriminate between these. Lower panel: Anisotropy (bed perpendicular /bed parallel resistivity) resulting from inversion of synthetic data generated using the thrust model, inverted with the dip angles from the anticline model. A low anisotropy zone similar to that observed in the real data inversion results from the incorrect dip assumption.

## REFERENCES

- Alvarez, P., A. Alvarez, L. MacGregor, F. Bolivar, R. Keirstead, and T. Martin, 2017, Reservoir properties prediction integrating controlled-source electromagnetic, prestack seismic, and well-log data using a rock-physics framework: Case study in the Hoop Area, Barents Sea, Norway, *Interpretation*, **5**, no. 2, SE43–SE60, doi: <https://doi.org/10.1190/INT-2016-0097.1>
- Bjorke, A. K., K. R. Hansen, and J. P. Morten, 2020, Recovering stratigraphy orientation using TTI 3D Gauss Newton inversion: SEG Technical Program Expanded Abstracts, 560–564, doi: <https://doi.org/10.1190/segam2020-3419985.1>.
- Hansen, K. R., M. Panzer, D. Shantsev, and R. Mittet, 2016, TTI inversion of CSEM data: SEG Technical Program Expanded Abstracts, 1014–1018, doi: <https://doi.org/10.1190/segam2016-13858558.1>.
- Hansen, K. R., M. Panzner, D. Shantsev, and K. Mohn, 2018, Comparison of TTI and VTI 3D inversion of CSEM data: 80th Conference and Exhibition, EAGE, Extended Abstracts, 1–5.
- Hoversten, G. M., R. L. Mackie, and Y. Hua, 2021, Reexamination of controlled-source electromagnetic inversion at the Lona prospect, Orphan Basin, Canada: *Geophysics*, **86**, E157–E170, doi: <https://doi.org/10.1190/geo2020-0538.1>.
- Karpiah, A. B., M. Meju, A. S. Saleh, P. M. Heng, P. S. Das, and N. Omar, 2022, Use of structure-guided 3D controlled-source electromagnetic inversion to map karst features in carbonates in offshore northwest Borneo: *Geophysics*, **87**, E279–E290, doi: <https://doi.org/10.1190/geo2021-0783.1>.
- Kho, J., M. Meju, R. V. Miller, and A. S. Saleh, 2024, Deep structural controls on the distribution of carbonate reservoirs and overburden heterogeneity in Central Luconia province, offshore Borneo revealed by 3D anisotropic inversion of regional controlled-source electromagnetic and magnetotelluric profile data: *Geophysics*, **89**, B17–B30, doi: <https://doi.org/10.1190/geo2023-0178.1>.
- Mackie, R. L., M. A. Meju, F. Miorelli, R. V. Miller, C. Scholl, and A. S. Saleh, 2020, Seismic image-guided 3D inversion of marine CSEM and MT data: *Interpretation*, **8**, no. 4, SS1–SS13, doi: <https://doi.org/10.1190/INT-2019-0266.1>.
- Meju, M., A. S. Saleh, A. B. Karpiah, P. S. Das, R. V. Miller, J. H. W. Kho, B. G. T. Alleyne, E. D. Rice-Oxley, and X. Legrand, 2024, Upper mantle flow and crustal deformation patterns beneath the Dangerous Grounds and Borneo where multiple plates converge in South China Sea revealed by 3-D anisotropic magnetotelluric imaging: *Geophysical Journal International*, **239**, no. 3, 1879–1899, doi: <https://doi.org/10.1093/gji/ggae346>.
- Saleh, A. S., M. Meju, R. L. Mackie, and E. Andersen, 2023, Seismic-electromagnetic projection attribute: Application in integrating seismic quantitative interpretation and 3D controlled-source electromagnetic-magnetotelluric broadband data inversion for robust ranking and sweet spotting of hydrocarbon prospects in offshore northwest Borneo: *Geophysics*, **88**, B329–B42, doi: <https://doi.org/10.1190/geo2022-0523.1>.
- Soyer, W., R. L. Mackie, S. Hallinan, F. Miorelli, A. Pavesi, S. Garanzini, B. Sagala, and H. Siagian, 2020, Geophysics over high enthalpy fields: Lessons from RLM-3D Magnetotelluric and Joint Inversions: Proceedings World Geothermal Congress 2020+1, Reykjavik, Iceland, April - October 2021.
- Weiland, T., 1977, A discretization method for the solution of Maxwell's equations for six-component fields: *Electronics and Communications AEU*, **31**, 116–120.
- Weiss, C. J., and G. A. Newman, 2002, Electromagnetic induction in a fully 3-D anisotropic earth: *Geophysics*, **67**, 1104–1114, doi: <https://doi.org/10.1190/1.1500371>.